Photo-stable Copper Nanoclusters: Compatible Förster Resonance Energy Transfer Assays and a Nano-thermometer

ARTICLE *in* JOURNAL OF PHYSICAL CHEMISTRY LETTERS · MARCH 2015

Impact Factor: 7.46 · DOI: 10.1021/acs.jpclett.5b00378

4 AUTHORS:

Subhadip Ghosh

Indian Institute of Science Education and Re…

12 PUBLICATIONS **57** CITATIONS

SEE PROFILE

Nirmal Kumar Das

Indian Institute of Science Education and Re…

6 PUBLICATIONS **7** CITATIONS

SEE PROFILE

Uttam Anand

University of Alberta

18 PUBLICATIONS **246** CITATIONS

SEE PROFILE

Saptarshi Mukherjee

Indian Institute of Science Education and Re…

49 PUBLICATIONS **639** CITATIONS

SEE PROFILE

THE JOURNAL OF PHYSICAL CHEMISTRY Letters

Letter

pubs.acs.org/JPCL

Photostable Copper Nanoclusters: Compatible Förster Resonance Energy-Transfer Assays and a Nanothermometer

Subhadip Ghosh,* Nirmal Kumar Das, Uttam Anand, and Saptarshi Mukherjee*

Department of Chemistry, Indian Institute of Science Education and Research Bhopal, Indore By-Pass Road, Bhauri, Bhopal 462 066, Madhya Pradesh, India

Supporting Information

ABSTRACT: To address the concern of material chemists over the issue of stability and photoluminescent (PL) characteristics of Cu nanoclusters (NCs), herein we present an efficient protocol discussing PL Cu NCs (Cu/HSA) having blue emission and high photostability. These PL NCs were illustrated as efficient probes for Förster resonance energy transfer (FRET) with a compatible fluorophore (Coumarin 153). Our spectroscopic results were well complemented by our molecular docking calculations, which also favored our proposed mechanism for Cu NC formation. The beneficial aspect and uniqueness of these nontoxic Cu/HSA NCs highlights their temperature-dependent PL reversibility as well as the reversible FRET with Coumarin 153, which enables them to be used as a nanothermometer and a PL marker for sensitive biological samples.

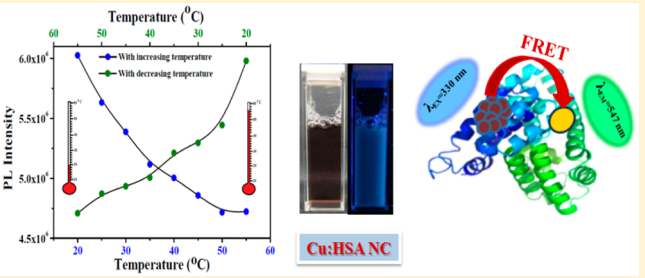

In the present era, growing interest has been mainly focused on noble metal nanoclusters (NCs) rather than nanoparticles (NPs) for various chemical and biological applications[1−4] primarily due to their advantage of exhibiting size-dependent optical properties, better water solubility, biocompatibility, and low toxicity.[5−8] On the basis of these excellent attributes, the noble metal NCs find numerous applications in optoelectronics, sensing, biolabeling, and clinical experiments of late.[9−11] In the past decade, Au and Ag NCs stabilized by biofriendly templates[12−14] have been the major thrust of researchers owing to their numerous applications as biological probes. In contrast, Cu NCs have been relatively less explored due to their low stability and ultrasmall size regime, which makes them prone to oxidation.[15−20] Metallic Cu is of severe biological importance;[21,22] hence, there is an utmost necessity to optimize the stability of Cu NCs, which could be a long-term solution for the drawbacks that it holds.

Förster resonance energy transfer (FRET) is a nonradiative energy-transfer process that can be applied to quantify the distance between two fluorophores, one acting as an energy donor and another as an energy acceptor.[23−25] The phenomenon of FRET is highly distance dependent and occurs only when the donor−acceptor separation is between 1 and 10 nm.[24] FRET is often used for monitoring structural/dynamic changes such as protein unfolding and refolding, DNA hybridization and cleavage, and binding of small fluorophores with various self-assembled systems.[23,25−27] There are earlier reports involving Au/Ag NCs as energy-transfer donors and acceptors with organic fluorophores or biomolecules;[27,28] however, Cu NCs due to their disadvantages as discussed earlier are seldom explored. Hence, it would be fairly challenging to investigate whether stable Cu NCs can be applied as FRET assays.

Thus, we carried out optimized synthesis of luminescent Cu NCs using human serum albumin (HSA) protein as a template. The Cu/HSA NCs exhibited superior photophysical properties close to the near-UV regime with the photoluminescent (PL) peak centered at 414 nm, a quantum yield (QY) of ∼4%, and a luminescent lifetime of 2.71 ns. The morphological insights of these NCs were analyzed using transmission electron microscopy (TEM), and subsequently, matrix-assisted laser desorption ionization time of flight (MALDI-TOF) spectral analyses revealed that 12 Cu atoms make up the core of the NCs. The time-dependent PL studies proved that the Cu/HSA NCs were fairly resistant to photodegradability for over a month, showing retention of their photophysical properties. Our PL experiments further corroborated that Cu/HSA NCs (donors) can efficiently exhibit FRET with a suitable pair, Coumarin153 (C-153 as acceptors, Scheme1).

The molecular docking calculations agreed very well with our results based on steady-state experiments. Further, our Cu/HSA NCs displayed a highly promising nanothermometric behavior; the PL intensity change exhibited a reversible phenomenon as a function of temperature (Scheme 1), and similar results were also obtained for the FRET experiments.

The Cu NCs were synthesized following an optimized one-pot route similar to the protocol as applied for Ag/HSA NCs[12] (Please see the Supporting Information (SI) for details). The

Received: February 21, 2015
Accepted: March 23, 2015

DOI: 10.1021/acs.jpclett.5b00378
J. Phys. Chem. Lett. 2015, 6, 1293−1298

Scheme 1. Schematic Representation Showing the Phenomenon of FRET and Nanothermometric Behavior Exhibited by the Cu/HSA NCs

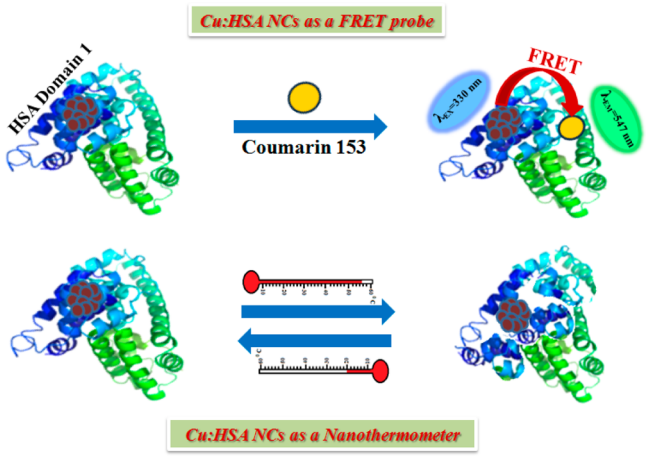

brownish violet solution of Cu/HSA NCs (Scheme S1, SI) showed a monotonic absorption plot without any clear band having an increased absorption below 330 nm (Figure S1, SI). On exciting these Cu/HSA NCs (λ_{ex} = 330 nm), the solution displayed a strong blue emission centered at 414 nm (Figure 1a).

In order to ensure that this emission peak corresponds to the most probable Cu/HSA NCs formed, we performed excitation-dependent emission studies with the NC solution (Figure S2, SI), which confirmed the spectral characteristics of Cu/HSA NCs. Time-resolved spectroscopic analysis of these Cu/HSA NCs exhibited an average luminescent lifetime of ~2.71 ns [1.10 ns (29.9%); 3.40 ns (70.1%)] (Figure 1b). The biexponential lifetime components can be attributed to the electronic transition between the filled d orbital and sp conduction bands.[18] The longer lifetime component most probably arises due to the transition between Cu ligands (in HSA), whereas the shorter component can be attributed to the Cu−Cu interaction.[29,30] The QY of the as-prepared NCs was estimated to be ~4% using C-153 as the reference.[31]

The luminescence properties in these NCs can be attributed to the templated scaffolding of Cu atoms by HSA (Scheme S1, SI).[5] This process of the stabilization of the Cu ions and the corresponding formation of the PL Cu NCs takes place as a function of time, as is evident from the time-dependent PL spectra (Figure S3, SI). The entrapped Cu^{2+} ions get slowly stabilized via electrostatic interactions with groups such as −OH, $-NH_2$, −COOH, −SH, and the bulky structure of HSA.[12] The tyrosine amino acid residues present in HSA reduce the Cu^{2+} ions to Cu atoms at an optimum pH ≈ 11.[12] To affirm that the luminescent properties exhibited by the Cu/HSA NCs are inherent characteristics of the NC and not arising from any oxidized counterparts in HSA,[32] we carried out control experiments in the presence of strong oxidant H_2O_2 (Figures S4−S6, SI). Addition of H_2O_2 resulted in the gradual quenching of the luminescent peak of Cu/HSA NCs due to oxidation of the Cu atomic cluster to Cu ions, thereby validating the formation of HSA template Cu NCs. In a seminal work, Pal and co-workers[18] using an analogous protein BSA as a template carried out similar control experiments and concluded that the blue emission is an inherent characteristic of the Cu_{QC}@BSA and does not arise from the oxidized metabolites of BSA. The Cu/HSA NCs also possess robust photostability, as is evident from the PL plot versus time (Figure S7, SI).

The MALDI-TOF mass spectrum of pure HSA shows a base peak at m/z = 66410 Da and a doubly charged peak at m/z = 33217 Da, whereas for the Cu/HSA NCs, the base peak and the corresponding doubly charged peaks were centered at m/z = 67137 and 33948 Da, respectively (Figure S8, SI). Comparing the differences between the two peaks for HSA and Cu/HSA NCs exemplified that the most stable atomic composition of the blue-emitting Cu/HSA NCs was 12 atoms. The Jellium model[6] ($E_{em} = E_{Fermi}/N^{0.33}$), a conventional theoretical model, was used to verify the atomic composition of the Cu NCs. From the respective values (E_{em} = 414 nm (2.995 eV) and E_{Fermi} of Cu, which is 7 eV), the number of atoms, N, was evaluated to be ~12.8, which is in agreement with the MALDI-TOF data. TEM analysis revealed that formation of the NCs has indeed taken place with a size regime of ~3 nm and exhibiting crystal lattice fringes (Figure S9, SI). Beside all of the previous characteristics, it was also confirmed that the Cu/HSA NCs are highly stable for over a month with almost complete retention in its PL properties, as is evident from the PL and time-resolved data (Figure S10, SI).

For the FRET experiment, we have selected C-153, an organic fluorescent dye molecule, as the acceptor having a very

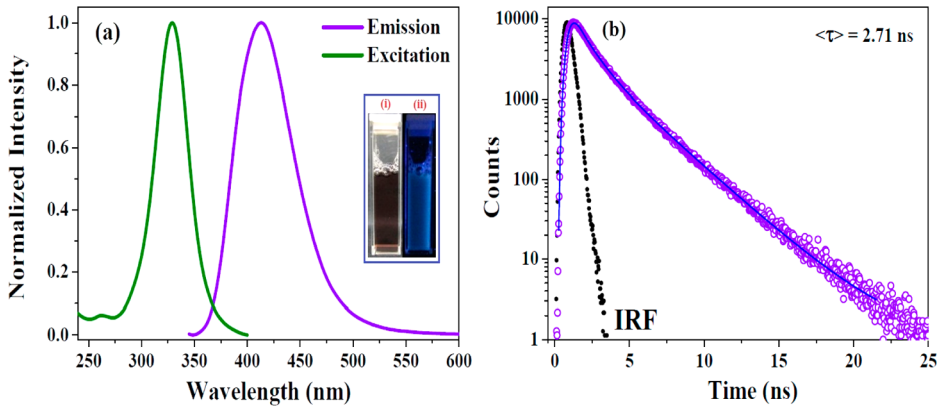

Figure 1. (a) The normalized PL excitation and emission spectra of the Cu/HSA NCs as marked in the figure. The inset shows the photographic images of the Cu/HSA NCs under (i) visible light and (ii) UV light (b). Representative PL lifetime decay profile (in logarithmic scale) of the Cu/HSA NCs.

DOI: 10.1021/acs.jpclett.5b00378
J. Phys. Chem. Lett. 2015, 6, 1293−1298

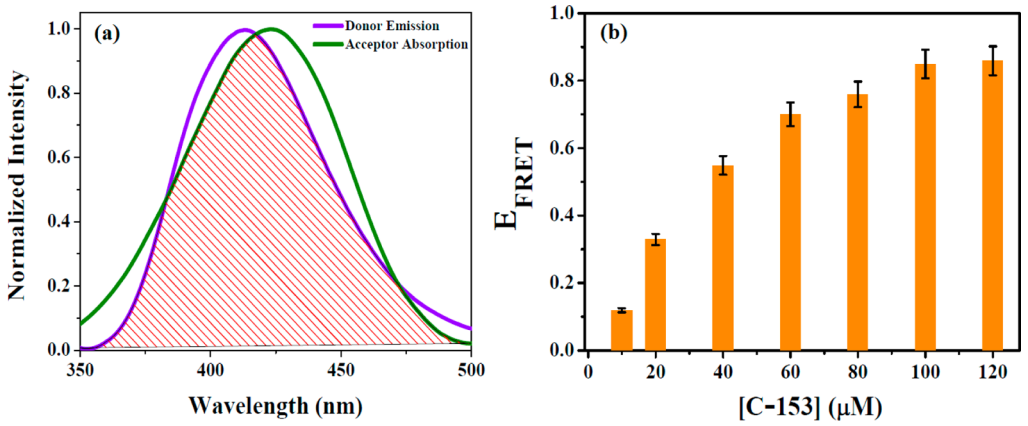

Figure 2. (a) Spectral overlap between normalized emission spectra of Cu/HSA NCs (donor) and the absorption spectra of C-153 (acceptor). (b) Histogram showing the variation of steady-state E_{FRET} against [C-153].

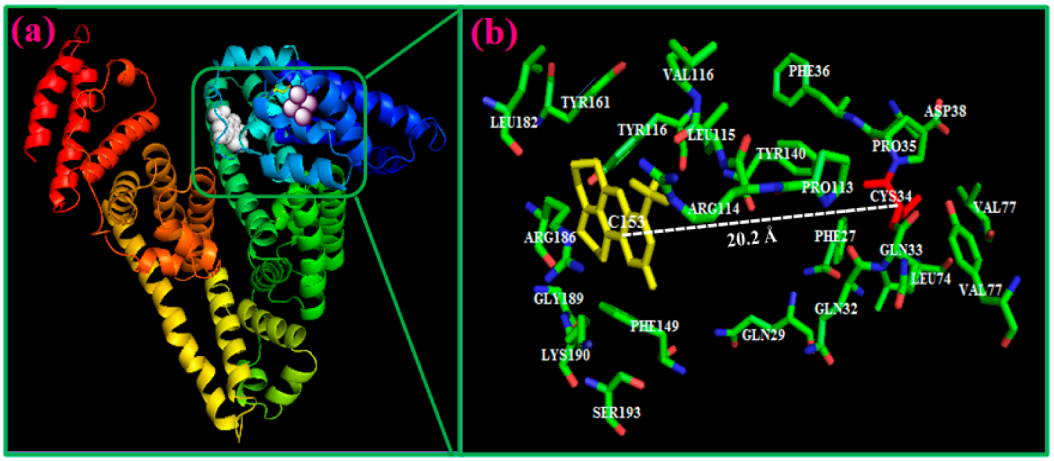

Figure 3. (a) Molecular docking results showing the minimum-energy conformations of the binding of C-153 in HSA and the plausible scaffold for the formation of Cu NCs. (b) Zoomed-in view that shows the amino acid residues present in the immediate vicinity of C-153 and the estimated distance between C-153 and Cys-34 (20.2 Å).

good spectral overlap with the Cu/HSA NCs (Figure 2a). C-153 is a strongly emissive dye whose spectral properties are sensitive to the environmental perturbations, making them ideal probes for deciphering heterogeneous environments.

For the FRET process to occur, it is important that the acceptor must not have any absorbance at the excitation wavelength of the donor (Figure S11, SI), and the PL emission of the acceptor (in the absence of donor) should be negligible at the donor excitation wavelength (Figure S12, SI). We have subjected the solution of Cu/HSA NCs with varying concentrations of C-153 ranging from 0 to 120 μM and recorded their emission profiles (λ_{ex} = 330 nm). It was observed that the PL peak for the Cu NCs showed gradual quenching with increasing concentrations of C-153, whereas the PL peak for C-153 exhibited incremental behavior (Figure S13, SI). Another important aspect for FRET is to have an estimation of the distance between Cu NCs and the C-153 molecules. From Figure 2b, the maximum steady-state FRET efficiency, E_{FRET} was obtained to be ~85%. The FRET distance, r, between Cu/HSA NCs and C-153 was evaluated to be ~18.6 Å (please see the SI for details), which falls well within the acceptable FRET limit[24] (Scheme 1). It must be mentioned here that in our system, we have observed Förster energy transfer ($1/r^6$ dependence) that is in analogy with other previous reports on noble metal NCs.[27,28] Mostly, in the case of metal NPs (larger in size than NCs and being nonemissive), the surface energy-transfer mechanism ($1/r^4$ dependence) operates when the donor−acceptor distance is smaller than the radius of the NP, whereas at larger distances, the energy-transfer mechanism follows FRET ($1/r^6$ dependence).[33] The time-resolved FRET studies revealed that the PL lifetimes of the Cu/HSA NCs exhibited a marginal decrement in the average lifetime values from 2.71 to 2.50 ns (Figure S14 and Table S1, SI), and the corresponding E_{FRET} was estimated to be ~8%. The significant differences between the E_{FRET} calculated from steady-state and time-resolved measurements indicates the interaction between the C-153 molecules and the Cu/HSA NCs to be a static quenching process. The Stern−Volmer analysis (Figure S15, SI) for the donor−acceptor interaction revealed the quenching constant, K_{SV}, to be 4.65×10^4 M^{-1} and the corresponding free energy to be ΔG = −9.18 kcal mol^{-1}, which indicates the interaction is spontaneous in nature.

To further substantiate the FRET studies, we have resorted to molecular docking calculations, a theoretical tool to study the interaction of guest molecules inside of the cavity of a host molecule.[25] From the docking calculations (please see the SI), the most probable binding site of C-153 was found to be subdomain IB of HSA (Figure 3a). The amino acid residues such as Leu182, Arg186, Gly189, Tyr116, Arg114, Phe149, and Lys190 present in the immediate vicinity of C-153 stabilize the

DOI: 10.1021/acs.jpclett.5b00378
J. Phys. Chem. Lett. 2015, 6, 1293−1298

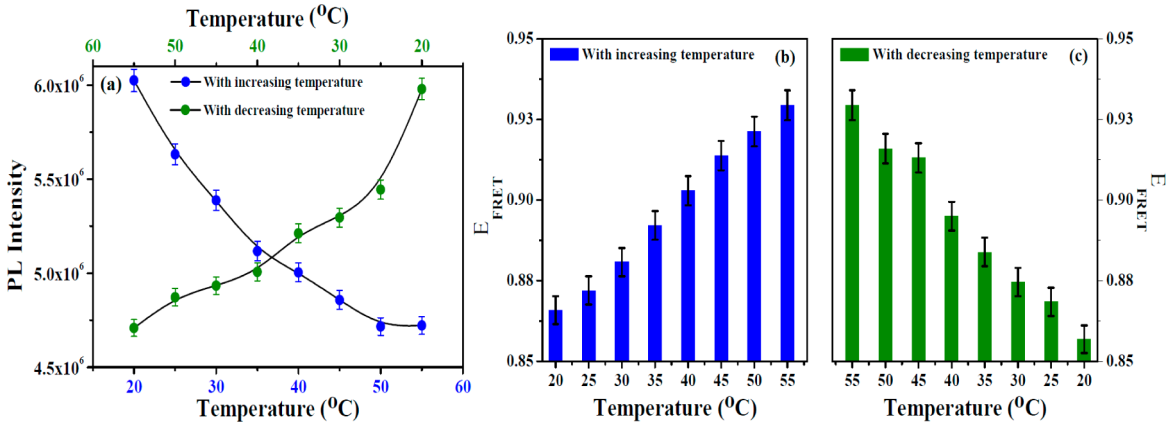

Figure 4. (a) Plot showing the PL reversibility exhibited by the Cu/HSA NCs as a function of temperature as marked in the figure. Histogram showing the variation of E_{FRET} with (b) increasing temperature and (c) decreasing temperature.

latter via hydrophobic and electrostatic interactions (Figure 3b).

Now, it has also been observed that the binding pocket of C-153 is close to the region where Cys-34 resides in HSA. Sarkar and co-workers[34] evaluated the distance between cyanine dyes and Cys-34 in BSA assuming that Au NCs were reported to reside in very close vicinity of Cys-34. Cu closely resembles Au in terms of chemical reactivity and noble character; hence, it is predominantly expected that the formation of Cu/HSA NCs would also take place in very close proximity of Cys-34. We emphasized earlier that tyrosine amino acids play the major role in the reduction of Cu^{2+} ions to Cu NCs, and from the PDB database of HSA,[35] it has been found that seven tyrosine residues reside in domain I of HSA. These results strongly support our proposed mechanism for Cu/HSA NC formation within protein scaffolds and indicate that domain I of HSA is the most probable site for the NC formation. Similarly, the estimated distance between C-153 (docked) and Cys-34 was found to be ∼20.2 Å (Figure 3b) from docking studies, which agrees very well with the experimentally obtained distance from our PL studies (∼18.6 Å). Further the free energy, ΔG(docking), was evaluated to be −7.05 kcal mol^{-1}, which is also in good agreement with the experimental value. Hence, the theoretical docking data clarifies the experimental evidence and supports our Cu/HSA NCs as compatible FRET assays.

In order to explore the thermal stability of the PL Cu/HSA NCs, we carried out PL experiments as a function of temperature. The PL intensity of the Cu/HSA NCs as expected exhibited quenching with increasing temperature (Figure S16a, SI) due to thermal instability/unfolding caused in the stabilizing scaffolds of HSA.[25] However, upon subjecting these unstable NCs to decreasing temperature (in exactly the reverse manner), it resulted in the complete restoration of its PL properties (Figure S16b, SI), which may be attributed to the regained rigidity of the stabilizing scaffolds. It must be noted here that the stabilizing template, HSA, also shows thermally induced unfolding−refolding in the similar temperature domain that can be directly related to the mechanism of temperature detection by our Cu/HSA NCs. Also, there is hardly any thermal hysteresis during the heating and cooling process of the Cu/HSA NCs, which indicates their versatility with respect to temperature (Figure S17, SI). The above results illustrate that our Cu/HSA NCs possess the unique ability of temperature-dependent PL reversibility and temperature detection capability (Figure 4a).

This lead us to the conjecture that our Cu/HSA NCs may have the capability of being applied in the emerging field of nanothermometry (Scheme 1).[36−38] Nanothermometry finds a wide variety of applications in nanoelectronics, nanophotonics, and biomedicine based on its capability to sense temperature fluctuations at the submicron scale.[36] Dynamics and reactivity of several biomolecular processes (e.g., heterogeneous cell heating) inside of cells are highly temperature governed.[37,38] Hence, our PL NCs can be highly beneficial for their dual advantages; they can be used in imaging as well as temperature sensing within a living cell. Further, inspired by the thermally reversible features exhibited by the Cu/HSA NCs, we tried to check whether these NCs showed similar FRET phenomenon. It was found that when Cu/HSA NCs were incubated with C-153 and the PL was monitored as a function of temperature, it indeed agreed to our envisaged idea and exhibited excellent temperature-dependent FRET. Most importantly, the FRET process was also found to be reversible with respect to temperature (Figure 4b,c). This trend can be ascribed to the fact that upon increasing temperature, the energy loss from the quenched NCs is manifested by the temporary transfer of energy to the acceptor mainly associated with the temperature-induced conformational changes in HSA, which is regained back by the NCs upon decreasing the temperature. This unique reversible FRET has rarely been reported to date and more precisely for a Cu NC.

In summary, our blue-emitting Cu/HSA NCs possess superior optical properties and photostability, as revealed from the various spectroscopic analyses. These Cu/HSA NCs proved themselves to be highly efficient FRET assays with an external probe, C-153, which serves as a compatible partner. The experimental findings were well-substantiated by our molecular docking calculations. The significance of Cu/HSA NCs as a nanothermometer and with promising reversible FRET behavior opens their applicability as biomarkers and for sensitive temperature detection, which has utmost priority in cell biology and biomedicine. We strongly believe that our NC assays, apart from being nontoxic, synthetically flexible, and cost-effective, can bloom in various interdisciplinary scientific investigations.

■ ASSOCIATED CONTENT

Supporting Information

Several spectroscopic analysis of the Cu/HSA NCs showing their morphological and photophysical properties are available.

DOI: 10.1021/acs.jpclett.5b00378
J. Phys. Chem. Lett. 2015, 6, 1293−1298

This material is available free of charge via the Internet at http://pubs.acs.org.

AUTHOR INFORMATION

Corresponding Authors

*E-mail: saptarshi@iiserb.ac.in (S.M.).
*E-mail: subhadipg@iiserb.ac.in (S.G.).

Notes

The authors declare no competing financial interest.

ACKNOWLEDGMENTS

We sincerely thank IISER Bhopal and the DST-Fast track scheme (No.: SR/FT/CS-19/2011) SERB for financial support. S.G. and N.K.D. thank UGC, and U.A. thanks CSIR, Govt. of India for providing fellowships. We sincerely thank Dr. Gajendra Saini, AIRF, JNU, New Delhi for helping us with the TEM experiments.

REFERENCES

(1) Chen, W.-T.; Hsu, Y.-J.; Kamat, P. V. Realizing Visible Photoactivity of Metal Nanoparticles: Excited-State Behavior and Electron-Transfer Properties of Silver (Ag_8) Clusters. *J. Phys. Chem. Lett.* **2012**, *3*, 2493−2499.

(2) Chen, L.-Y.; Wang, C.-W.; Yuan, Z.; Chang, H.-T. Fluorescent Gold Nanoclusters: Recent Advances in Sensing and Imaging. *Anal. Chem.* **2015**, *87*, 216−229.

(3) Stamplecoskie, K. G.; Kamat, P. V. Size-Dependent Excited State Behavior of Glutathione Capped Gold Clusters and Their Light-Harvesting Capacity. *J. Am. Chem. Soc.* **2014**, *136*, 11093−11099.

(4) Ghosh, S.; Anand, U.; Mukherjee, S. Investigating the Evolution of Drug Mediated Silver Nanoparticles. *Analyst* **2013**, *138*, 4270−4274.

(5) Xie, J.; Zheng, Y.; Ying, J. Y. Protein-Directed Synthesis of Highly Fluorescent Gold Nanoclusters. *J. Am. Chem. Soc.* **2009**, *131*, 888−889.

(6) Zheng, J.; Zhang, C. W.; Dickson, R. M. Highly Fluorescent, Water-Soluble, Size-Tunable Gold Quantum Dots. *Phys. Rev. Lett.* **2004**, *93*, 077402.

(7) Retnakumari, A.; Setua, S.; Menon, D.; Ravindran, P.; Muhammed, H.; Pradeep, T.; Nair, S.; Koyakutty, M. Molecular-Receptor-Specific, Non-Toxic, Near-Infrared-Emitting Au Cluster−Protein Nanoconjugates for Targeted Cancer Imaging. *Nanotechnology* **2010**, *21*, 055103.

(8) Wang, H.-H.; Lin, C. -A. J.; Lee, C.-H.; Lin, Y.-C.; Tseng, Y.-M.; Hsieh, C.-L.; Chen, C.-H.; Tsai, C.-H.; Hsieh, C.-T.; Shen, J.-L.; et al. Fluorescent Gold Nanoclusters as a Biocompatible Marker for In Vitro and In Vivo Tracking of Endothelial Cells. *ACS Nano* **2011**, *5*, 4337−4344.

(9) Ghosh, S.; Anand, U.; Mukherjee, S. Luminescent Silver Nanoclusters Acting as a Label-Free Photoswitch in Metal Ion Sensing. *Anal. Chem.* **2014**, *86*, 3188−3194.

(10) Hu, D.; Sheng, Z.; Fang, S.; Wang, Y.; Gao, D.; Zhang, P.; Gong, P.; Ma, Y.; Cai, L. Folate Receptor-Targeting Gold Nanoclusters as Fluorescence Enzyme Mimetic Nanoprobes for Tumor Molecular Colocalization Diagnosis. *Theranostics* **2014**, *4*, 142−153.

(11) Guével, X. L.; Spies, C.; Daum, N.; Jung, G.; Schneider, M. Highly Fluorescent Silver Nanoclusters Stabilized by Glutathione: A Promising Fluorescent Label for Bioimaging. *Nano Res.* **2012**, *5*, 379−387.

(12) Anand, U.; Ghosh, S.; Mukherjee, S. Toggling Between Blue- and Red-Emitting Fluorescent Silver Nanoclusters. *J. Phys. Chem. Lett.* **2012**, *3*, 3605−3609.

(13) Yu, J.; Patel, S. A.; Dickson, R. M. In Vitro and Intracellular Production of Peptide-Encapsulated Fluorescent Silver Nanoclusters. *Angew. Chem., Int. Ed.* **2007**, *46*, 2028−2030.

(14) Venkatesh, V.; Shukla, A.; Sivakumar, S.; Verma, S. Purine-Stabilized Green Fluorescent Gold Nanoclusters for Cell Nuclei Imaging Applications. *ACS Appl. Mater. Interfaces* **2014**, *6*, 2185−2191.

(15) Wei, W.; Lu, Y.; Chen, W.; Chen, S. One-Pot Synthesis, Photoluminescence, and Electrocatalytic Properties of Subnanometer-Sized Copper Clusters. *J. Am. Chem. Soc.* **2011**, *133*, 2060−2063.

(16) Kawasaki, H.; Kosaka, Y.; Myoujin, Y.; Narushima, T.; Yonezawa, T.; Arakawa, R. Microwave-Assisted Polyol Synthesis of Copper Nanocrystals without Using Additional Protective Agents. *Chem. Commun.* **2011**, *47*, 7740−7742.

(17) Cao, H.; Chen, Z.; Zheng, H.; Huang, Y. Copper Nanoclusters as a Highly Sensitive and Selective Fluorescence Sensor for Ferric Ions in Serum and Living Cells by Imaging. *Biosens. Bioelectron.* **2014**, *62*, 189−195.

(18) Goswami, N.; Giri, A.; Bootharaju, M. S.; Xavier, P. L.; Pradeep, T.; Pal, S. K. Copper Quantum Clusters in Protein Matrix: Potential Sensor of Pb^{2+} Ion. *Anal. Chem.* **2011**, *83*, 9676−9680.

(19) Ma, J.-Y.; Chen, P.-C.; Chang, H.-T. Detection of Hydrogen Sulfide through Photoluminescence Quenching of Penicillamine−Copper Nanocluster Aggregates. *Nanotechnology* **2014**, *25*, 195502.

(20) Fernández-Ujados, M.; Trapiella-Alfonso, L.; Costa-Fernández, J.; Pereiro, R.; Sanz-Medel, A. One-Step Aqueous Synthesis of Fluorescent Copper Nanoclusters by Direct Metal Reduction. *Nanotechnology* **2013**, *24*, 495601.

(21) Bertini, I.; Gray, H. B.; Lippard, S. J.; Valentine, J. S. *Bioinorganic Chemistry*; University Science Books: Mill Valley, CA, 1994.

(22) Festa, R. A.; Thiele, D. J. Copper: An Essential Metal in Biology. *Curr. Biol.* **2011**, *21*, R877−R883.

(23) Lakowicz, J. R. *Principles of Fluorescence Spectroscopy*; Kluwer Academic: New York, 1999.

(24) Hevekerl, H.; Spielmann, T.; Chmyrov, A.; Widengren, J. Förster Resonance Energy Transfer beyond 10 nm: Exploiting the Triplet State Kinetics of Organic Fluorophores. *J. Phys. Chem. B* **2011**, *115*, 13360−13370.

(25) Das, N. K.; Ghosh, N.; Kale, A. P.; Mondal, R.; Anand, U.; Ghosh, S.; Tiwari, V.; Kapur, M.; Mukherjee, S. Temperature Induced Morphological Transitions from Native to Unfolded Aggregated States of Human Serum Albumin. *J. Phys. Chem. B* **2014**, *118*, 7267−7276.

(26) Fisher, C. A.; Narayanaswami, V.; Ryan, R. O. The Lipid-Associated Conformation of the Low Density Lipoprotein Receptor Binding Domain of Human Apolipoprotein E. *J. Biol. Chem.* **2000**, *275*, 33601−33606.

(27) Xiao, Y.; Shu, F.; Wong, K.-Y.; Liu, Z. Förster Resonance Energy Transfer-Based Biosensing Platform With Ultrasmall Silver Nanoclusters as Energy Acceptors. *Anal. Chem.* **2013**, *85*, 8493−8497.

(28) Raut, S.; Rich, R.; Fudala, R.; Butler, S.; Kokate, R.; Gryczynski, Z.; Luchowskic, R.; Gryczynski, I. Resonance Energy Transfer between Fluorescent BSA Protected Au Nanoclusters and Organic Fluorophores. *Nanoscale* **2013**, *6*, 385−391.

(29) Guével, X. L.; Hötzer, B.; Jung, G.; Hollemeyer, K.; Trouillet, V.; Schneider, M. Formation of Fluorescent Metal (Au, Ag) Nanoclusters Capped in Bovine Serum Albumin Followed by Fluorescence and Spectroscopy. *J. Phys. Chem. C* **2011**, *115*, 10955−10963.

(30) Wen, X.; Yu, P.; Toh, Y.-R.; Hsu, A.-C.; Lee, Y.-C.; Tang, J. Fluorescence Dynamics in BSA-Protected Au_{25} Nanoclusters. *J. Phys. Chem. C* **2012**, *116*, 19032−19038.

(31) Rurack, K.; Spieles, M. Fluorescence Quantum Yields of a Series of Red and Near-Infrared Dyes Emitting at 600−1000 nm. *Anal. Chem.* **2011**, *83*, 1232−1242.

(32) Goswami, N.; Makhal, A.; Pal, S. K. Toward an Alternative Intrinsic Probe for Spectroscopic Characterization of a Protein. *J. Phys. Chem. B* **2010**, *114*, 15236−15243.

(33) Saini, S.; Srinivas, G.; Bagchi, B. Distance and Orientation Dependence of Excitation Energy Transfer: From Molecular Systems to Metal Nanoparticles. *J. Phys. Chem. B* **2009**, *113*, 1817−1832.

(34) Banerjee, C.; Kuchlyan, J.; Banik, D.; Kundu, N.; Roy, A.; Ghosh, S.; Sarkar, N. Interaction of Gold Nanoclusters with IR Light Emitting Cyanine Dyes: A Systematic Fluorescence Quenching Study. *Phys. Chem. Chem. Phys.* **2014**, *16*, 17272−17283.

DOI: 10.1021/acs.jpclett.5b00378
J. Phys. Chem. Lett. 2015, 6, 1293−1298

(35) Sugio, S.; Kashima, A.; Mouchizuki, S.; Noda, M.; Kobayashi, K. Crystal Structure of Human Serum Albumin at 2.5 Å Resolution. *Protein Eng.* **1999**, *12*, 439−446.
(36) Chen, X.; Essner, J. B.; Baker, G. A. Exploring Luminescence-Based Temperature Sensing Using Protein-Passivated Gold Nanoclusters. *Nanoscale* **2014**, *6*, 9594−9598.
(37) Shang, L.; Stockmar, F.; Azadfar, N.; Nienhaus, G. U. Intracellular Thermometry by Using Fluorescent Gold Nanoclusters. *Angew. Chem., Int. Ed.* **2013**, *52*, 11154−11157.
(38) Yang, J.-M.; Yang, H.; Lin, L. Quantum Dot Nano Thermometers Reveal Heterogeneous Local Thermogenesis in Living Cells. *ACS Nano* **2011**, *5*, 5067−5071.

DOI: 10.1021/acs.jpclett.5b00378
J. Phys. Chem. Lett. 2015, 6, 1293−1298